

Preliminary Simulations of FLR effects on RFP tearing modes.

Charlson C. Kim and the NIMROD Team

Plasma Science and Innovation Center
University of Washington, Seattle

August 24, 2007

Abstract. Preliminary simulations of finite Larmor radius (FLR) effects on $m = 1$ tearing instabilities in a reverse field pinch (RFP) plasma are presented. δf particle-in-cell (PIC) simulations were performed by extending a hybrid drift kinetic-MHD model to include the full Lorentz equations of motion to take into account FLR effects. The simulations show that for an idealized phase space distribution, sufficiently energetic ions stabilize the tearing mode. These simulations show good agreement with analytic theory and demonstrate the FLR physics capability of the hybrid kinetic-MHD model.

Key words: tearing modes–FLR effects–hybrid kinetic-MHD simulation

1 Introduction

Current driven tearing modes play a key role in the dynamics of RFP experiments, both in sustaining the configuration and as a key mechanism to many disruptive instabilities[1]. Extensive efforts—experimental, theoretical, and computational—have been expended in understanding and controlling tearing mode instabilities and their impact on RFP plasmas. Three key areas where tearing modes play an essential role are the sawtooth oscillation, field line stochasticization, and mode locking. Tearing modes are believed to be the triggering mechanism in sawtooth oscillations observed in RFPs[2]. Nonlinear interaction of several tearing modes is believed to drive the $m = 0$ edge mode that leads to the sawtooth crash. Overlapping tearing islands are also known to lead to stochastic field lines which can significantly degrade confinement[2]. Tearing islands are also believed to result in resistive wall mode locking[3]. The mode locking “brakes” the plasma rotation, significantly reducing the dynamo and leading to premature termination of the plasma.

The control and mitigation of tearing mode instabilities in RFPs are crucial to its success as a confinement device. One proposed mechanism for the stabilization of tearing modes is through FLR effects from energetic ions[4], e.g. from neutral beams. Analysis by Svidzinski et al. has shown that tearing modes can be stabilized with sufficiently energetic ions. The stabilizing influence is found to increase with increasing energy, i.e. increasing Larmor radius. Svidzinski’s analysis derives the dielectric response of the fast ions. A perturbative method is employed to assess the impact of individual terms from the dielectric tensor on the resistive eigenmode equation. Through this analysis, it is found that the dominant stabilizing term is unique to an anisotropic distribution function. Also of significance is a term related to the transit time magnetic pumping. The analytic treatment is limited in that the distribution function is approximated by a δ function in velocity.

This paper will present preliminary results from our computational study of the impact of an energetic minority ion population on tearing mode stability. We employ a hybrid kinetic-MHD model implemented in the NIMROD code[5,6]. We extend a drift kinetic particle module[7] to include Lorentz equations of motion to

capture the FLR effects. With this model we show stabilization of the tearing mode by FLR effects in agreement with the analytic theory. In the subsequent sections we will outline the hybrid kinetic-MHD model, the parameters for the simulation, present our results, then conclude with a brief discussion.

2 Hybrid Kinetic-MHD Model

The hybrid kinetic-MHD equations are solved in the NIMROD code. The hybrid kinetic-MHD model captures kinetic effects that are absent in the usual MHD fluid equations with minor modification. In the limit of a low density energetic minority ion species, the only modification to the MHD equations is the addition of the divergence of the energetic particle pressure tensor to the center of mass (COM) momentum equation. The resistive MHD equations that we solve are

$$mn \left(\frac{\partial \mathbf{V}}{\partial t} + \mathbf{V} \cdot \nabla \mathbf{V} \right) = \mathbf{J} \times \mathbf{B} + \nabla \cdot \rho \nu \nabla \mathbf{V} - \nabla \cdot \mathbf{p}_h \quad (1)$$

$$\frac{\partial \mathbf{B}}{\partial t} = -\nabla \times \mathbf{E} + \kappa_{divb} \nabla \nabla \cdot \mathbf{B} \quad (2)$$

$$\mathbf{J} = \frac{1}{\mu_0} \nabla \times \mathbf{B} \quad (3)$$

$$\mathbf{E} = -\mathbf{V} \times \mathbf{B} + \eta \mathbf{J} \quad (4)$$

where we have explicitly included the kinematic viscosity and excluded the MHD fluid pressure ($\beta_{MHD} = 0$) in the momentum equation. The additional term in Faraday's law controls $\nabla \cdot \mathbf{B}$ errors where κ_{divb} is a parameter that adjusts the strength of the diffusion. The dynamic equations (1), (2) for the fields \mathbf{V} and \mathbf{B} are closed by constitutive equations (3), (4) for \mathbf{J} and \mathbf{E} , i.e. Ampere's law and Ohm's law. The reader is referred to references[5, 6] for details of NIMROD the code.

The drift kinetic δf PIC model[7] has been extended to incorporate the effects of Lorentz force particles to capture the necessary FLR effects for the study of tearing mode stabilization. The Lorentz equations of motion

$$\begin{aligned} \dot{\mathbf{x}} &= \mathbf{v} \\ \dot{\mathbf{v}} &= \frac{q}{m} (\mathbf{E} + \mathbf{v} \times \mathbf{B}) \end{aligned} \quad (5)$$

are advanced using the Boris push[8]. The particle pressure tensor is computed by taking moments of the δf PIC marker particles[9]

$$\delta \mathbf{p}(\mathbf{x}) = \int m \mathbf{v} \mathbf{v} \delta f(\mathbf{x}, \mathbf{v}) d^3 v \quad (6)$$

$$= \sum_{i=1}^N m \mathbf{v}_i \mathbf{v}_i \delta f_i \delta(\mathbf{x} - \mathbf{x}_i) \quad (7)$$

where the sum is over all particles, the subscript i denotes the marker particle quantities, the COM velocity of the energetic particles is assumed to be zero, and δf is the particle weight.

The δf PIC method reduces the discrete statistical noise associated with conventional particle methods by augmenting the usual Lagrangian phase space sampling with control variates and importance sampling[10]. Control variates and importance sampling are common tools utilized in Monte Carlo integration[11, 12]. The additional computational cost of δf arises from advancing an addition variable, the phase space "weight", along the phase space characteristic $\dot{\mathbf{z}}$

$$\dot{\delta f} = -\dot{\mathbf{z}} \cdot \frac{\partial f_{eq}}{\partial \mathbf{z}} \quad (8)$$

where $\mathbf{z} = (\mathbf{x}, \mathbf{v})$ is the phase space coordinate, $\dot{\mathbf{z}} = \dot{\mathbf{z}} - \dot{\mathbf{z}}_{eq}$ is the perturbed phase space trajectory, $\dot{\mathbf{z}}_{eq}$ is the trajectory evaluated with equilibrium field quantities, f_{eq} is the equilibrium distribution function, and the over-dots indicate time derivatives. The crux of the δf method lies in choosing the appropriate equilibrium distribution function that satisfies

$$\dot{\mathbf{z}}_{eq} \cdot \frac{\partial f_{eq}}{\partial \mathbf{z}} = 0. \quad (9)$$

For the Lorentz characteristics of equation (5) the equilibrium distribution that satisfies the constraint of equation (9) is

$$f_{eq} = f(\mathbf{x}, v^2) + \frac{1}{\omega_c} (\mathbf{v} \cdot \mathbf{b} \times \nabla f) \quad (10)$$

where ω_c is the ion cyclotron frequency and \mathbf{b} is the unit direction of the magnetic field. The second term is necessary to satisfy stationarity in the presence of fast FLR gyro-motion[13].

3 Simulation Parameters

Single helicity linear tearing mode simulations were performed using an alpha model equilibrium $\nabla \times \mathbf{B} = \lambda(r)\mathbf{B}$ where

$$\lambda(r) = 2\Theta \left[1 - \left(\frac{r}{a} \right)^{\alpha_0} \right]. \quad (11)$$

The RFP simulation domain is approximated by a straight cylinder with minor radius $a = .5\text{m}$, $B_0 = .3\text{T}$, $\Theta = 1.75$, $\alpha_0 = 3$, density $n = 1 \times 10^{19}\text{m}^{-3}$, magnetic Lundquist number $S = 1 \times 10^4$, and axial mode number $ka = 2$. These parameters correspond to case A in [4]. Without FLR effects, we compute a linear growth rate of $\gamma\tau_A = 1.3 \times 10^{-3}$, where $\tau_A = a/v_A$.

The energetic ion density is $n_h \exp \left[- \left(\frac{r}{0.45a} \right)^2 \right]$ with $n_h = 2 \times 10^{-17}\text{m}^{-3}$. To compare with the analytic theory, we load a $\delta(v_\perp - v_0)$ function in velocity and consider only the perpendicular velocity component contributions to the particle pressure tensor. The particle orbits are sub-cycled to accommodate the disparity in time step constraints between the particles and the fluid.

4 Simulation Results

Linear simulations of tearing modes with FLR effects modeled by δf PIC show good agreement with the analytic theory. As with the analytic theory, we see a strong stabilizing effect with increasing Larmor radius as shown in table (1). The tearing mode is nearly stabilized at $L/a = .35$ where L is the Larmor diameter and a is the minor radius.

Table 1. Increasing particle velocity and corresponding ratio of Larmor diameter to minor radius show significant reduction of normalized tearing mode growth rate.

$v_0(\text{m/s})$	L/a	$\gamma\tau_A$
base case	-	1.3×10^{-3}
1.0×10^6	.14	1.0×10^{-3}
1.5×10^6	.21	5.4×10^{-4}
2.0×10^6	.28	1.5×10^{-4}
2.5×10^6	.35	5.1×10^{-5}

We examine the $L/a = .21$ case where the growth rate has been decreased by a factor of 2. From the simulations, we observe that the ratio of magnetic mode energy to kinetic mode energy decreases dramatically from $\mathcal{O}(1)$ in the absence of FLR effects to $\mathcal{O}(10^{-2})$ for $L/a = .21$. However, the topology of the magnetic eigenmode is unaltered from the case without FLR effects. The mode structure of the velocity field tangential to the flux surfaces is substantially altered as is seen from figure (1) and figure (2). These figures show the $ka = 2, m = 1$ axial component of the velocity field eigenmode. For comparison we show the usual resistive tearing mode without FLR effects. The contour on the left in figure (1) and the solid line profile in figure (2) show the characteristic localized mode structure of a resistive tearing instability without FLR effects. The addition of FLR effects broaden the velocity eigenmode—shown in the contour on the right in figure (1) and the dashed profile of figure (2)—to fill an appreciable fraction of the domain and eliminate the dipolar profile characteristic of the resistive eigenmode. Work continues to understand the significance of this change in mode topology and energy balance.

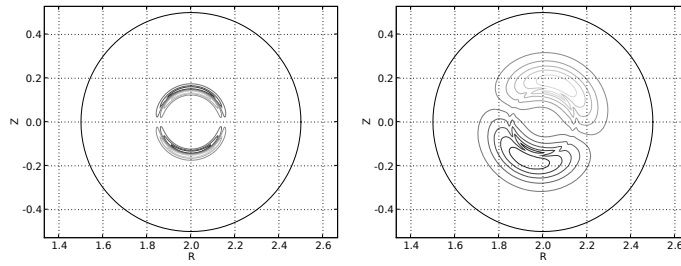


Fig. 1. V_ϕ contours of linear tearing mode. Characteristic $m = 1$ resistive tearing mode (left) is significantly altered by FLR effects (right). Dark circle at $r = .5\text{m}$ is simulation boundary.

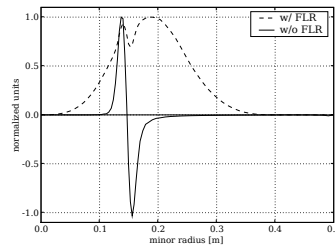


Fig. 2. Profiles of eigenmodes from figure 1 show strong impact of FLR effects on eigenmode. Amplitudes have been normalized for comparison.

5 Conclusion

The Lorentz force extensions of the hybrid kinetic-MHD model implemented in NIMROD reproduce the linear stabilization predicted by Svidzinski et al.. In agreement with the analytic theory, we see an increasing stabilizing effect as the velocity of minority ions is increased with stabilization occurring when the Larmor diameter exceeds $1/3$ the minor radius. This corresponds to hydrogen ions with an energy of $\sim 20\text{keV}$.

The inclusion of FLR effects dramatically alters the velocity eigenmode structure to a broader profile while maintaining the magnetic mode structure. A dramatic reduction in ratio of magnetic energy to kinetic energy as the Larmor radius is increased has also been observed.

With the capabilities of the hybrid kinetic-MHD model demonstrated, we continue in extending to more realistic parameters and models, particularly more realistic phase space distribution functions and the full particle pressure tensor. Initial simulations indicate that the stabilizing effects are greatly reduced as was conjectured in reference[4].

References

1. S. C. Prager et al., Nuclear Fusion **45**, (2005) S276
2. S. Ortolani and D. D. Schnack, *Magnetohydrodynamics of Plasma Relaxation* (World Scientific, Singapore, 1993)
3. R. Fitzpatrick et al., Physics of Plasmas **6**, (1999) 3878
4. V. A. Svidzinski and S. C. Prager, Physics of Plasmas **11**, (2004) 980
5. C. R. Sovinec et al., Journal of Computational Physics **195**, (2004) 355
6. D. D. Schnack et al., Physics of Plasmas **13**, (2006) 058103
7. C. C. Kim et al., Computer Physics Communications **164**, (2004) 448
8. C. K. Birdsall and A. B. Langdon, *Plasma physics via computer simulation* (Adam Hilger, Bristol, England, 1991)
9. S. E. Parker and W. W. Lee, Physics of Fluids **B 5**, (1993) 77
10. A. Y. Aydemir, Physics of Plasmas **1**, (1994) 822
11. N. Metropolis et al., Journal of Chemical Physics **21**, (1953) 1087
12. W. H. Press et al., *Numerical Recipes in C - The Art of Scientific Computing* (Cambridge University Press, Cambridge, MA, 1992)
13. M. N. Rosenbluth and N. Rostoker, Physics of Fluids **2**, (1959) 23